Bad Metallic Transport in a Modified Hubbard Model

Connie H. Mousatov, Ilya Esterlis, and Sean A. Hartnoll

Bad metallic transport in a modified Hubbard model

Connie H. Mousatov, Ilya Esterlis, Sean A. Hartnoll

Department of Physics, Stanford University,
Stanford, California, USA

Strongly correlated metals often display anomalous transport, including T-linear resistivity above the Mott-Ioffe-Regel limit. We introduce a tractable microscopic model for bad metals, by restoring in the well-known Hubbard model — with hopping t and on-site repulsion U — a 'screened Coulomb' interaction between charge densities that decays exponentially with spatial separation. This interaction lifts the extensive degeneracy in the spectrum of the $t = 0$ Hubbard model, allowing us to fully characterize the small t electric, thermal and thermoelectric transport in our strongly correlated model. Throughout the phase diagram we observe T-linear resistivity above the Mott-Ioffe-Regel limit, together with strong violation of the Weidemann-Franz law and a large thermopower that can undergo sign change.

Introduction. — In conventional metals, electrical resistance arises from the microscopic scattering of electronic quasiparticles. This paradigm is challenged in bad metals, where the resistivity grows with temperature above the Mott-Ioffe-Regel (MIR) limit [1]. Such behavior is widely observed in strongly correlated materials at high temperatures [2, 3], and hints at non-quasiparticle transport which must be understood along radically different lines than traditional Boltzmann theory.

High temperature, bad metallic regimes of strongly correlated materials are often far from the battleground of multiple low temperature competing orders. Indeed, bad metals exhibit similarities across many materials, including an often noted T-linear resistivity [4]. Despite suggestive universal behavior, and some success reproducing this behavior numerically using methods such as dynamical mean field theory (DMFT) [5–8], the understanding of bad metals has been hampered by the lack of a microscopic, theoretical model in which the resistivity can be computed in a transparent way without artificial control parameters. To this end, we introduce a realistic modification of the widely-studied Hubbard model for correlated electrons that allows us to obtain explicit results for high temperature, non-quasiparticle, bad metal transport.

The model. — We will study the lattice Hamiltonian

$$H = t \sum_{\langle ij \rangle, s} c_{is}^\dagger c_{js} + U \sum_i n_{i\uparrow} n_{i\downarrow} + \frac{V}{2} \sum_{i \neq j} e^{-|\vec{x}_i - \vec{x}_j|/\ell} \, n_i n_j \, . \tag{1}$$

As usual the density $n_i = \sum_s c_{is}^\dagger c_{is}$, with $s \in \{\uparrow, \downarrow\}$ the fermion spin. The positions $\vec{x}_i = a\vec{\imath}$ form a two dimensional square lattice. The first two terms in (1) comprise the usual Hubbard model, with hopping t over nearest neighbours $\langle ij \rangle$ and on-site repulsion U. The final 'screened Coulomb' interaction is short range, but not strictly finite range. Such terms are dropped in the conventional on-site Hubbard model (which has $V = 0$), and also from finite range extensions thereof, and are essential

for our results. The precise functional form of the interaction does not qualitatively affect our results. Restoring these terms allows us to obtain explicit and finite results for transport coefficients in the weak hopping regime $t \ll \{k_B T, U, V\}$. Here T is the temperature. These temperatures are higher than those of most observed bad metals; they pertain instead to recent transport experiments in cold atomic gases [9]. In condensed matter these conditions may be realized in, for example, oxide thermoelectrics [10] and magic angle graphene bilayers [11]. Our immediate objective is rather to obtain controlled and physically transparent bad metal transport.

Small t transport in the Hubbard model has been studied in a number of works [10, 12]. However, the spectrum of the Hubbard model with $t = 0$ is extremely degenerate, with excitations occupying either the single-site upper or lower Hubbard band. In contrast, the new interaction in the model (1) — that is exponentially localized to within a microscopic range ℓ but not strictly finite range — is sufficient to split the extensive degeneracy of the $t = 0$ theory (spin degeneracy remains, but will play no role in our discussion). This allows us to use conventional non-degenerate perturbation theory in small t to obtain a low energy spectral density, and hence transport coefficients, that are finite in the infinite volume limit.

All of the terms in the U and V interactions in (1) commute. This means that all computations in small t perturbation theory can be evaluated using *classical* Monte Carlo simulations in the $t = 0$ theory. This statistical description of bad metal transport is an immense simplification. The statistical regime is intrinsically incoherent and distinct from Boltzmann-Drude theory, as emphasized in [13]. Using classical Monte Carlo, we are able to work with a large system size in two dimensions, and furthermore study the entire filling range $0 \leq n \leq 2$ and obtain the full thermoelectric conductivity matrix.

The conductivity. — To leading order at small hopping t, the conductivity is computed as follows. At $t = 0$, occupation number configurations $\{n\}$ define eigenstates of

charge $N_{\{n\}} = e \sum_{is} n_{is}$ and energy $E_{\{n\}} = \frac{1}{2} \sum_{is} n_{is} \epsilon_{is}$, with on-site energies $\epsilon_{is} = U n_{i\bar{s}} + V \sum_{j \neq i} e^{-|\vec{x}_i - \vec{x}_j|/\ell} n_j$. Here $n_{i\bar{s}}$ is the number of electrons at site i with opposite spin to s. Using classical Monte Carlo simulation, typical configurations $\{n\}$ are generated for a given temperature and filling [14]. The real and dissipative electrical conductivity is a weighted sum over these configurations

$$\sigma_1(\omega) = \frac{2e^2}{h} \frac{(\pi a t)^2}{\hbar \, \text{vol}} f(\omega) \sum_{\{n\}} \frac{e^{-\beta(E_{\{n\}} - \mu N_{\{n\}})}}{\mathcal{Z}} \sum_{i,s} \Delta_{is}(\omega) \,. \tag{2}$$

Here vol is the volume and $f(\omega) = (1 - e^{-\beta\hbar\omega})/\hbar\omega$. The inverse temperature $\beta \equiv 1/(k_B T)$ and the partition function $\mathcal{Z} = \sum_{\{n\}} e^{-\beta(E_{\{n\}} - \mu N_{\{n\}})}$. Given a configuration, the spectral weight $\Delta_{is}(\omega)$ counts the number of excitations with energy $\hbar\omega$ that can be generated with a single hop between neighbouring sites. $\Delta_{is}(\omega)$ has units of inverse frequency and is defined precisely in the Supplementary Material. Analogous formulae exist for the thermoelectric conductivity α and the thermal conductivity κ, and are also given in the Supplementary Material.

The expression (2) is strictly only valid for $\hbar\omega \gtrsim t$. At lower frequencies non-perturbative localization physics could potentially deplete the density of states $\Delta_{is}(\omega)$. This concern is addressed in a later section. We proceed to use (2) to obtain dc transport observables.

Figure 1 shows a representative occupation number configuration, together with the corresponding on-site energies $\epsilon_{i\uparrow}$. Differences of neighboring on-site energies determine $\Delta_{is}(\omega)$ and hence the optical conductivity, also shown in the figure. The conductivity is computed using 15000 weighted configurations in (2). The optical conductivity displays transitions between lower and upper 'Hubbard bands' together with a low frequency conductance peak. In the $t = 0$ Hubbard model, the optical conductivity is a sum of delta functions at $\omega = 0, \pm U$. In Figure 1 these peaks have been broadened, leading to a finite dc conductivity. This occurs because the exponentially localized interaction V, with any range $\ell > \ell_\star \approx 1.76a$, lifts the extensive degeneracy of the $t = 0$ Hubbard model, as we show in the Supplementary Material. This is the only essential property of the interaction.

The low frequency peak in figure 1 is Gaussian, in contrast to a conventional Lorentzian Drude peak. A Gaussian peak is also seen in the high temperature expansion of a hard boson model [15], and indicates that the energy differences contributing to $\sigma(\omega)$ are essentially random.

Transport results. — We will work throughout with the values $V = 0.1U$ and $\ell = 2a$. Thus the exponential interaction is microscopically short range and the small value of V means that results can be compared meaningfully to the Hubbard model. The hopping $t \ll \{U, V, k_B T\}$.

The resistivity for $t \ll k_B T \lesssim U$ is shown for various fillings in figure 2. Away from the Mott insulating upturn at $n = 1$, the resistivity is approximately T-linear, with some weak curvature at lower temperatures. The
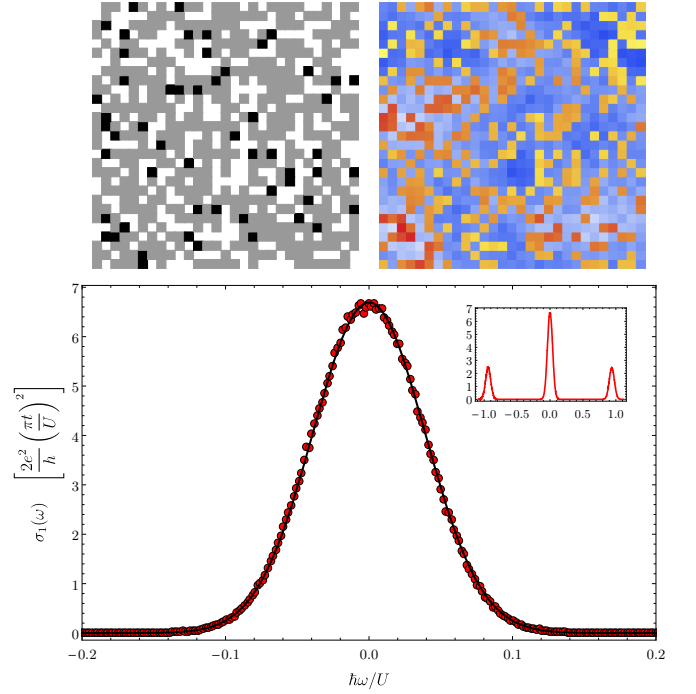

FIG. 1. On-site energies for a typical configuration with a 29×29 lattice at temperature $k_B T = 0.76U$, coupling $V = 0.1U$, range $\ell = 2a$ and filling $n = 0.63$. Top left shows the occupation numbers for the configuration (white is unoccupied, gray is singly-occupied and black is doubly-occupied). Top right shows the on-site potentials for up spins, $\epsilon_{i\uparrow}$, generated by this configuration. A broadened upper (red/yellow) and lower (blue) Hubbard band are seen. Bottom shows the corresponding low frequency conductance peak. The solid line shows a fit to a Gaussian. The inset shows the optical conductivity over a wider frequency range, including transitions between the lower and upper Hubbard bands.

magnitude of the resistivity is $\rho \sim h/e^2 \times U^2/t^2 \gg h/e^2$ throughout, so the system is a bad metal.

Themoelectric and thermal transport are usefully quantified by the thermopower $S \equiv \alpha/\sigma$ and Lorenz ratio $L \equiv \kappa/(\sigma T)$, respectively. Figure 4 shows the Lorenz ratio for $t \ll k_B T \lesssim U$. Strong violation of the Weidemann-Franz (WF) law is seen across the entire phase diagram: $L \ll L_0$, the Sommerfeld value, almost everywhere, except for just above the Mott regime, where $L \gg L_0$. The WF law is not expected to hold at these high temperatures, but L_0 remains a useful yardstick for the relative efficacy of thermal and charge transport. The thermopower is shown in the Supplementary Material, and displays behavior widely seen in e.g. DMFT studies of strongly correlated systems [16–19]: large values $S \sim k_B/e$ and changes in sign as a function of temperature.

At the highest temperatures $k_B T \gg U, V$ our numerical results are in excellent agreement with known expressions for the standard on-site Hubbard model [10, 12, 20]. We summarize these results in the Supplementary Material. The salient features are an exact T-linear resistivity,
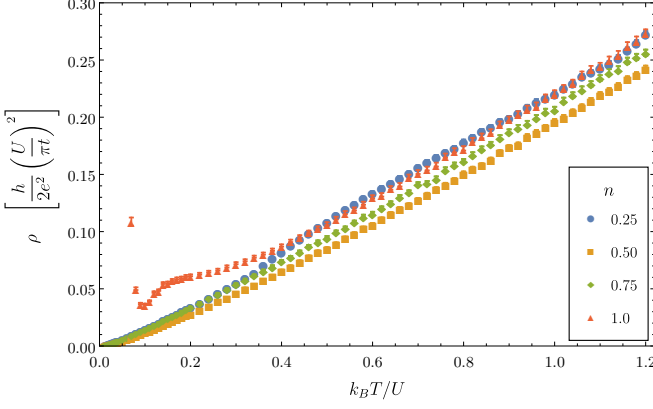
FIG. 2. Resistivity as a function of temperature. Statistical errors are shown.
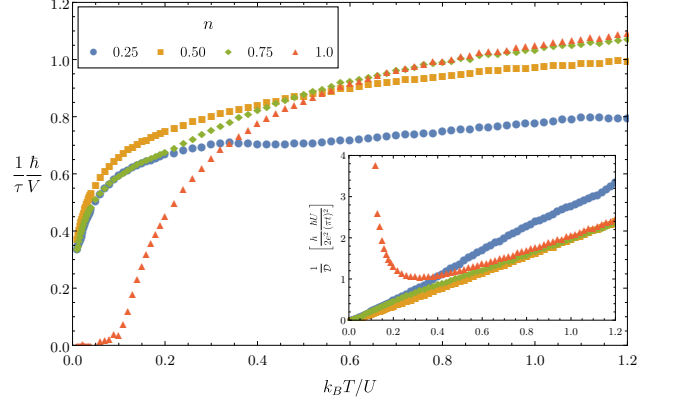

FIG. 3. Current relaxation rate as a function of temperature. Inset: Inverse Drude weight as of function of temperature. The statistical uncertainty in the fit to (3) is negligible.

a temperature-independent thermopower S and a Lorenz ratio $L \sim 1/T^2$. These limiting behaviors are largely independent of the interactions [4, 17, 21, 22].

Origin of T-linear resistivity.— The Gaussian zero frequency peak in $\sigma(\omega)$ can be fit to

$$\sigma_1(\omega) = \mathcal{D}\tau \, e^{-\pi(\tau\omega)^2} \, . \qquad (3)$$

Thus τ is the current relaxation or transport lifetime. The resistivity is $\rho = 1/(\mathcal{D}\tau)$. The 'Drude weight' $\mathcal{D}$ is the area under the low frequency conductance peak. It is best thought about as follows. The total kinetic energy of all electrons can be written $K_{\rm tot} \equiv \int_{-\infty}^{\infty} \sigma_1(\omega)d\omega$ [23]. The ratio $\mathcal{D}/K_{\rm tot}$ therefore measures the reduction of the conductance peak kinetic energy due to interactions. In our incoherent regime, the spectral weight $\mathcal{D}$ corresponds to the kinetic energy of hopping processes with a small potential energy transition.

Figure 3 shows the current relaxation rate $1/\tau$ as a function of temperature. The relaxation rates all saturate to a constant of order $V/\hbar$ at high T. The V interaction is responsible for the finite transport lifetime at small t, whereas in the Hubbard model this lifetime must be generated nonperturbatively in t. Away from half filling, the relaxation rate becomes only mildly temperature-dependent below $k_BT \sim U$ and remains nonzero at the lowest temperatures we have probed [24]. The approximate T-linearity of the resistivity over this temperature range is instead controlled by the kinetic energy of low energy hopping processes, which exhibits a strong temperature dependence $\mathcal{D} \sim t^2/T$, shown in the inset of figure 3. The decrease of $\mathcal{D}$ with increasing temperature is due to increasingly random single particle kinetic energies of both signs, that tend to cancel. We expect the low temperature divergence in $\mathcal{D}$ to be cut off below $T \sim t$, crossing over to the Fermi liquid value $\mathcal{D} \sim t$.

Figure 4 shows the ratio $\mathcal{D}/K_{\rm tot}$ across the phase diagram. The values of $\mathcal{D}/K_{\rm tot} \sim 0.4 - 0.6$ seen in the proximity of the Mott regime are characteristic of those
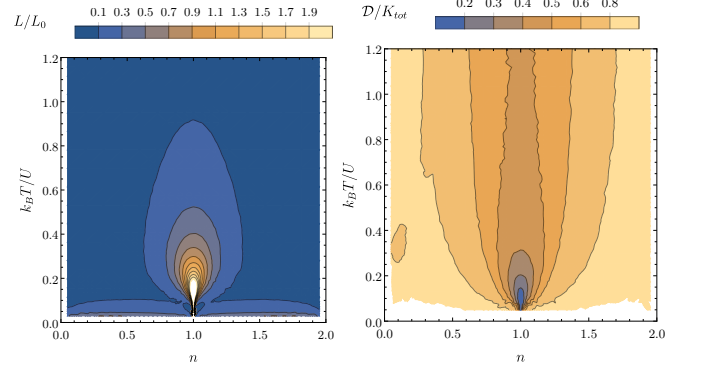
observed in strongly correlated metals [23].

FIG. 4. Left: Violation of the Weidemann-Franz law across the phase diagram. The Sommerfeld value $L_0 \equiv \pi^2/3 \times (k_B/e)^2$. Right: Fraction of the electronic kinetic energy in the conductance peak — as measured by $\mathcal{D}/K_{\rm tot}$.

Distinct bad metal regimes.— Hidden under the featureless T-linear resistivity lies a crossover in behavior at $k_BT \sim U$. There are in fact two bad metallic regimes in the model; temperatures $k_BT \lesssim U$ are physically distinct from the infinite temperature limit. This can be seen by considering the diffusivity.

In the small t regime it is necessary to consider coupled charge and heat diffusion. There are three conductivities σ, α and κ and three associated thermodynamic susceptibilities: $\chi \equiv -e^2 \, \partial^2 f/\partial\mu^2$, $\zeta \equiv -e \, \partial^2 f/\partial T\partial\mu$ and $c_\mu \equiv -T \, \partial^2 f/\partial T^2$, as well as the specific heat at fixed charge $c_n \equiv c_\mu - T\zeta^2/\chi$. These determine two independent diffusivities $D_\pm$ by [4]: $D_+ D_- = \sigma/\chi \cdot \kappa/c_n$ and $D_+ + D_- = \sigma/\chi + \kappa/c_n + T(\zeta\sigma - \chi\alpha)^2/(c_n\chi^2\sigma)$. Figure 5 shows the diffusivity D_+ as a function of temperature for several fillings. The behavior of D_- is similar. The diffusivities are temperature-dependent below $k_BT \sim U$ but constant at high temperatures. We have extended
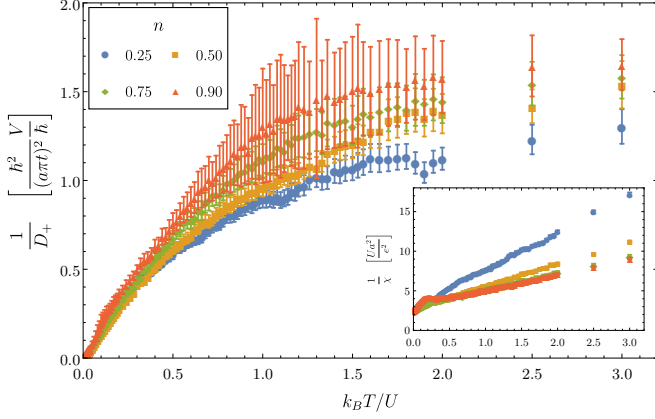
FIG. 5. Inverse diffusivity against temperature. The larger errors bars on the diffusivity are due to a near-cancellation in the computation of κ and c_n, see Supplementary Material. Inset: Inverse susceptibility against temperature.

the temperature range to make the saturation clearer.

The susceptibilities also exhibit crossovers at $k_B T \sim U$. For example, the charge compressibility χ is well-described by $1/\chi = a + b\,T/U$, for doping-dependent coefficients a and b. See inset of figure 5. The nontrivial temperature dependence of the diffusivities and thermodynamic susceptibilities conspire to cancel out of the electrical resistivity, whose approximately T-linear behavior is featureless across $k_B T \sim U$, as found in [9, 25].

The high temperature behavior of $D_\pm$ follows from the Hubbard model formulae collected in the Supplementary Material: $D_\pm = c_\pm \tau (a\pi t)^2/\hbar^2 \left[1 + \mathcal{O}(V/U)\right]$, with $c_+ = 2/\pi$ and $c_- = n(2-n)/\pi$. Recall that τ is temperature-independent at high temperatures. Writing $D_\pm \lesssim \frac{1}{2} v^2 \tau$, these expressions reveal the expected 'Lieb-Robinson'-like microscopic operator growth velocity of $v \sim a\pi t/\hbar$, in the sense of [26]. At temperatures $k_B T \lesssim U$, the effective velocity $v_{\text{eff}}^2 \equiv 2D_+/\tau$ becomes temperature dependent, tracking the temperature dependence of the kinetic energy $\mathcal{D}$, discussed above.

Origin of bad metallic transport.— Figure 1, top right, shows an interaction-induced, emergent disordered landscape of on-site potentials. The current decay rate is set by the strength of inhomogeneities in this landscape: $1/\tau \sim \Delta\epsilon \sim V/\hbar$. The separation of scales $t \ll U, V$ implies that the landscape evolves slowly, and is static on the timescale of current decay. Therefore, while momentum is microscopically relaxed by umklapp-like electronic interactions, transport is effectively controlled by local hops in an inhomogeneous potential. The usual arguments for a Mott-Ioffe-Regel bound are thus inapplicable because current is not carried by delocalized excitations with a well-defined momentum. This is the same reason that the bound does not apply to free electrons in a disordered background potential, and raises the concern that our interacting model may similarly exhibit localization.

Indeed, we noted above that the small t perturbative computation of the conductivity is not strictly valid for low frequencies $\omega \in (-t, t)$. We will not exclude the possibility that a gap opens in this frequency range, analogously to how the Mott argument leads to a soft gap for strongly disordered free electrons [27]. Interactions can reduce the strength of the Mott argument due to an increased many-body phase space [28]. Most importantly, however, even if such many-body localization does occur in our model, it is fragile and can be destroyed by coupling to physical degrees of freedom that have been omitted for simplicity in the model. As a proof of concept, we show in the Supplementary Material that coupling our model to phonons with a Debye scale ω_0 and dimensionless electron-phonon coupling g smears out any low frequency gap if $t \ll \sqrt{g\,\omega_0\,k_B T} \ll U, V, k_B T$, while leaving our transport results intact.

Discussion.— Recent transport measurements in a cold-atomic realization of the Hubbard model with $0 \le k_B T \lesssim U$ and $t \ll U$ show remarkable similarities with our results [9]. As we have found, the experiments show a nontrivial temperature dependence of the diffusivity and charge susceptibility, that cancel out to produce a close to T-linear resistivity. The individual temperature dependence and magnitude of these quantities are all similar to those that we have found. This suggests that, at least for temperatures $k_B T \gtrsim t$, our V interaction captures similar physics to a nonperturbative treatment of t in the on-site Hubbard model. Indeed, our results are also in agreement with the trends observed in Quantum Monte Carlo simulation of transport in a Hubbard model [25] over a similar temperature range, with real time transport behavior inferred from the Euclidean data [29]. A smoking gun signature of our picture for transport is the emergent disordered landscape predicted in our model. It should be possible to directly observe this landscape using local probes in cold atom experiments or, perhaps more easily, in full quantum monte carlo simulations.

Finally, a hierarchy between the current decay rate and the single particle bandwidth also underpins an interesting recent body of work on strange and bad metals in large N models [30–36] and DMFT [5–8]. Several of these approaches share the feature of our model that the conductivity is controlled by a single-particle electronic spectral function describing rapid electron decay into an inert 'bath'. In our case the single-particle decay is caused by the emergent disordered landscape.

ACKNOWLEDGEMENTS

———————

[1] V. J. Emery and S. A. Kivelson, Phys. Rev. Lett. **74**, 3253 (1995).

[2] O. Gunnarsson, M. Calandra, and J. E. Han, Rev. Mod. Phys. **75**, 1085 (2003).

[3] N. E. Hussey, K. Takenaka, and H. Takagi, Philosophical Magazine **84**, 2847 (2004).

[4] S. A. Hartnoll, Nature Phys. **11**, 54 (2015), arXiv:1405.3651 [cond-mat.str-el].

[5] X. Deng, J. Mravlje, R. Žitko, M. Ferrero, G. Kotliar, and A. Georges, Phys. Rev. Lett. **110**, 086401 (2013).

[6] J. Vučičević, D. Tanasković, M. J. Rozenberg, and V. Dobrosavljević, Phys. Rev. Lett. **114**, 246402 (2015).

[7] W. Ding, R. Žitko, P. Mai, E. Perepelitsky, and B. S. Shastry, Phys. Rev. B **96**, 054114 (2017).

[8] W. Ding, R. Žitko, and B. S. Shastry, Phys. Rev. B **96**, 115153 (2017).

[9] P. T. Brown, D. Mitra, E. Guardado-Sanchez, R. Nourafkan, A. Reymbaut, S. Bergeron, A.-M. S. Tremblay, J. Kokalj, D. A. Huse, P. Schauss, and W. S. Bakr, (2018), arXiv:1802.09456 [cond-mat.quant-gas].

[10] S. Mukerjee and J. E. Moore, Applied Physics Letters **90**, 112107 (2007).

[11] Y. Cao, V. Fatemi, S. Fang, K. Watanabe, T. Taniguchi, E. Kaxiras, and P. Jarillo-Herrero, Nature **556**, 43 (2018), article.

[12] G. Beni, Phys. Rev. B **10**, 2186 (1974).

[13] S. Mukerjee, V. Oganesyan, and D. Huse, Phys. Rev. B **73**, 035113 (2006).

[14] See Supplemental Material [url] for technical details, which includes Refs. [37–39].

[15] N. H. Lindner and A. Auerbach, Phys. Rev. B **81**, 054512 (2010).

[16] T. Pruschke, M. Jarrell, and J. Freericks, Advances in Physics **44**, 187 (1995).

[17] G. Pálsson and G. Kotliar, Phys. Rev. Lett. **80**, 4775 (1998).

[18] J. Merino and R. H. McKenzie, Phys. Rev. B **61**, 7996 (2000).

[19] V. Zlatić, G. R. Boyd, and J. K. Freericks, Phys. Rev. B **89**, 155101 (2014).

[20] P. M. Chaikin and G. Beni, Phys. Rev. B **13**, 647 (1976).

[21] J. Kokalj, Phys. Rev. B **95**, 041110 (2017).

[22] E. Perepelitsky, A. Galatas, J. Mravlje, R. Žitko, E. Khatami, B. S. Shastry, and A. Georges, Phys. Rev. B **94**, 235115 (2016).

[23] D. N. Basov, R. D. Averitt, D. van der Marel, M. Dressel, and K. Haule, Rev. Mod. Phys. **83**, 471 (2011).

[24] At temperatures $k_B T \ll V$, we expect charge ordering away from half filling. Indeed, working with larger values of $V \sim U$, strong features in the low temperature specific heat are seen at commensurate fillings of $n = \frac{1}{2}, \frac{1}{4}, \cdots$, at which CDW ordering occurs. The spins remain disordered (even at $n = 1$) because the U and V interactions only depend on the charge density. This low temperature physics will change once t is treated beyond perturbation theory and is furthermore unrelated to our discussion of bad metallicity, so we have not studied it in detail.

[25] E. W. Huang, R. Sheppard, B. Moritz, and T. P. Devereaux, arXiv:1806.08346 [cond-mat.str-el].

[26] T. Hartman, S. A. Hartnoll, and R. Mahajan, Phys. Rev. Lett. **119**, 141601 (2017), arXiv:1706.00019 [hep-th].

[27] N. F. Mott and E. A. Davis, The Philosophical Magazine: A Journal of Theoretical Experimental and Applied Physics **17**, 1269 (1968).

[28] S. Gopalakrishnan, M. Müller, V. Khemani, M. Knap, E. Demler, and D. A. Huse, Phys. Rev. B **92**, 104202 (2015).

[29] S. Lederer, Y. Schattner, E. Berg, and S. A. Kivelson, Proceedings of the National Academy of Sciences **114**, 4905 (2017).

[30] S. A. Hartnoll, A. Lucas, and S. Sachdev, MIT press (2018), arXiv:1612.07324 [hep-th].

[31] O. Parcollet and A. Georges, Phys. Rev. B **59**, 5341 (1999).

[32] X.-Y. Song, C.-M. Jian, and L. Balents, Phys. Rev. Lett. **119**, 216601 (2017).

[33] A. A. Patel, J. McGreevy, D. P. Arovas, and S. Sachdev, (2017), arXiv:1712.05026 [cond-mat.str-el].

[34] D. Chowdhury, Y. Werman, E. Berg, and T. Senthil, (2018), arXiv:1801.06178 [cond-mat.str-el].

[35] Y. Werman and E. Berg, Phys. Rev. B **93**, 075109 (2016).

[36] Y. Werman, S. A. Kivelson, and E. Berg, npj Quantum Materials **2**, 7 (2017).

[37] I. Paul and G. Kotliar, Phys. Rev. B **67**, 115131 (2003).

[38] J. Crossno, J. K. Shi, K. Wang, X. Liu, A. Harzheim, A. Lucas, S. Sachdev, P. Kim, T. Taniguchi, K. Watanabe, T. A. Ohki, and K. C. Fong, Science **351**, 1058 (2016).

[39] G. D. Mahan, *Many-particle physics* (Springer Science & Business Media, 2013).